Metabolic Brain Disease (2019) 34:1565–1575
https://doi.org/10.1007/s11011-019-00464-7

ORIGINAL ARTICLE

Novel mutations in SLC16A2 associated with a less severe phenotype of MCT8 deficiency

Silvia Masnada[1,2] · Stefan Groenweg[3] · Veronica Saletti[4] · Luisa Chiapparini[5] · Barbara Castellotti[6] · Ettore Salsano[7] · W. Edward Visser[3] · Davide Tonduti[1,4]

Received: 18 April 2019 / Accepted: 8 July 2019 / Published online: 22 July 2019

Abstract

Mutations in the thyroid hormone transporter MCT8 cause severe intellectual and motor disability and abnormal serum thyroid function tests, a syndrome known as MCT8 deficiency (or: Allan-Herndon-Dudley syndrome, AHDS). Although the majority of patients are unable to sit or walk independently and do not develop any speech, some are able to walk and talk in simple sentences. Here, we report on two cases with such a less severe clinical phenotype and consequent gross delay in diagnosis. Genetic analyses revealed two novel hemizygous mutations in the *SLC16A2* gene resulting in a p.Thr239Pro and a p.Leu543Pro substitution in the MCT8 protein. In vitro studies in transiently transfected COS-1 and JEG-3 cells, and ex vivo studies in patient-derived fibroblasts revealed substantial residual uptake capacity of both mutant proteins (Leu543Pro > Thr239Pro), providing an explanation for the less severe clinical phenotype. Both mutations impair MCT8 protein stability and interfere with proper subcellular trafficking. In one of the patients calcifications were observed in the basal ganglia at the age of 29 years; an abnormal neuroradiological feature at this age that has been linked to untreated (congenital) hypothyroidism and neural cretinism. Our studies extend on previous work by identifying two novel pathogenic mutations in *SLC16A2* gene resulting in a mild clinical phenotype.

Keywords MCT8 · Leukoencephalopathy · Cerebral calcifications · MCT8 deficiency · Thyroid hormone · Thyroid hormone transporter

Silvia Masnada, Stefan Groenweg, W. Edward Visser and Davide Tonduti contributed equally to this work.

✉ Davide Tonduti
davidetondu@hotmail.com

1 Pediatric Neurology Unit, V. Buzzi Children's Hospital, Via Castelvetro 32, 20154 Milan, Italy

2 Department of Brain and Behavioural Sciences, University of Pavia, Pavia, Italy

3 Department of Internal Medicine, Academic Center for Thyroid Diseases, Erasmus MC, University Medical Center, CN Rotterdam, The Netherlands

4 Child Neurology Department, IRCCS Foundation C. Besta Neurological Institute, Milan, Italy

5 Neuroradiology Unit, IRCCS Foundation C. Besta Neurological Institute, Milan, Italy

6 Unit of Genetics of Neurodegenerative and Metabolic Diseases, IRCCS Foundation C. Besta Neurological Institute, Milan, Italy

7 Unit of Neurodegenerative and Neurometabolic Rare Diseases, IRCCS Foundation C. Besta Neurological Institute, Milan, Italy

Introduction

Thyroid hormone (TH) is crucial for the development of many tissues, in particular the brain, and it regulates energy metabolism throughout life (Yen 2001). The thyroid gland mainly produces the pro-hormone thyroxine (T4) and a small amount of the active hormone 3,3′,5-tri-iodothyronine (T3). Most effects of TH are exerted through binding of T3 to the nuclear thyroid hormone receptors (TRs) (Yen et al. 2006). The amount of T3 available for receptor action in TH-target tissues is tightly regulated by the de-iodinating enzymes (Gereben et al. 2008). Since TH action and metabolism take place inside the target cells, it needs to cross the cell membrane for which TH transporter proteins are required (Hennemann et al. 2001). The most specific TH transporter identified to date is the monocarboxylate transporter (MCT)8 (Friesema et al. 2003). Mutations in the *SLC16A2* gene, which encodes MCT8, have been associated with MCT8 deficiency (also known as: Allan-Herndon-Dudley syndrome, AHDS), characterized by severe intellectual and motor disability and abnormal serum thyroid

function tests comprising elevated serum T3 concentrations, low serum (free) T4 concentrations and a (high-) normal TSH concentration (Friesema et al. 2004; Dumitrescu et al. 2004). Compiling evidence suggests that MCT8 is essential for the transport of TH across the blood-brain-barrier and into different cell-types inside the brain (Vatine et al. 2017; Mayerl et al. 2014). Therefore, it has been widely accepted that MCT8 deficiency results in a hypothyroid state in the brain which impairs prenatal and post-natal brain development. In addition, the elevated serum T3 concentrations render tissues that rely on transporters other than MCT8 thyrotoxic (Groeneweg et al. 2016), contributing to the very low body weight, tachycardia and muscle wasting observed in patients with MCT8 deficiency.

Over the last decades an increasing number of patients harboring different genetic mutations have been reported (summarized in (Groeneweg et al. 2017b)). The majority of patients present severe cognitive impairment, hypotonia, signs of pyramidal and extrapyramidal involvement, together contributing to the poor head control and inability to sit or stand independently. Neuro-imaging usually reveals a severe delay in myelination which is, by definition, mostly pronounced in the first years of life (Tonduti et al. 2013; Matheus et al. 2015). However, a small subset of patients present a relatively mild clinical phenotype and are able to walk and talk in simple words (e.g.(Stevenson et al. 1990, Schwartz et al. 2005, Vaurs-Barriere et al. 2009, Visser et al. 2009, Novara et al. 2017)). Limited clinical and molecular information is available for this subgroup of MCT8 deficiency. Here, we report on two of such patients, harboring two different novel hemizygous missense mutations in MCT8, and extend on the currently available clinical characteristics of MCT8 deficiency.

Materials and methods

[^{125}I]T_3 and [^{125}I]T_4 were synthesized as described previously (Mol and Visser 1985). Unlabeled iodothyronines, silychristin, bovine serum albumin (BSA), and D-glucose were obtained from Sigma-Aldrich (Zwijndrecht, The Netherlands [NL]); culture dishes from Corning (Schiphol, NL); culture medium from Invitrogen (Bleiswijk, NL); transfection reagent X-tremeGENE 9 from Roche Diagnostics (Almere, NL); 4–20% gradient Mini-PROTEAN TGX Precast Protein Gel from from Bio-Rad (Veenendaal, NL), polyvinylidene difluoride membranes and NuPAGE 4x lithium dodecyl sulfate loading buffer from Thermo Fisher Scientific (Bleiswijk, NL). Rabbit polyclonal antibody HPA003353 against human SLC16A2 amino acids 75 to 155 from Sigma Aldrich (Manufacturer: Atlas Antibodies, Stockholm; RRID AB_1079343); mouse monoclonal glyceraldehyde-3-phosphate dehydrogenase (GAPDH) antibody Mab 374 from Merck Millipore (Amsterdam, NL; RRID AB_2107445); IRDye680-labeled goat anti-rabbit IgG (RRID AB_621843) and IRDye800-labeled goat anti-mouse IgG antibodies (RRID AB_10706161) from LI-COR (Leusden, NL); mouse monoclonal ZO-1 antibody from Invitrogen (RRID:AB_2533147). Alexa Fluor 488-labeled goat anti-rabbit IgG (RRID AB_143165) and Alexa Fluor 633-labeled goat anti-mouse IgG antibodies (RRID AB_2535718) from Thermo Fisher Scientific; Vectashield H-1200 containing DAPI from Brunschwig (Amsterdam, NL).

Genetic analyses

Genomic DNA was extracted from peripheral blood lymphocytes, according to a standard procedure. Written informed consent for DNA analysis was obtained from all patients and family members. DNA samples were screened for mutations in the *SLC16A2* gene (Xq13.2). Exons and intron–exon boundaries (exons 1–6) were analyzed by direct sequence analysis using an automated sequencing system (ABI 3130 XL). The primers are available on request. Nucleotides and amino acid residues were numbered according to the reference gene sequence of the transcript GenBank (NCBI): *SLC16A2* (*Homo sapiens* NM_006517.3, NP_006508.2). Sequence variations and predicted protein changes were described according to nomenclature recommendations (http://www.hgvs.org/mutnomen/recs.html). Segregation of genetic variants was analyzed through validation in all available family members. Frequencies of novel missense variants were determined by comparison with The Human Gene Mutation Database (http://www.hgmd.cf.ac.uk/ac/index.php), the NCBI dbSNP132ver (http://www.ncbi.nlm.nih.gov/projects/SNP/) and the Exome Variant Server (http://evs.gs.washington.edu/EVS/). In silico analysis of missense variants was performed using the PolyPhen-2 (http://genetics.bwh.harvard.edu/pph2/), and SIFT prediction test (http://sift.jcvi.org/).

Plasmids and cloning

The cloning of human MCT8 into pcDNA3 and of human CRYM into pSG5 expression vectors has been previously described (Friesema et al. 2006; Friesema et al. 2008). CRYM is an intracellular high-affinity TH-binding protein that prevents the efflux of internalized TH. The p.Thr239Ala, p.Thr239Ala, p.Leu543Pro and p.Leu543Ala mutations were introduced using QuikChange site-directed mutagenesis according to manufacturer's protocol (Stratagene, Amsterdam, NL; primer sequences available upon request). The presence of the intended mutations was verified by Sanger sequencing of the complete cDNA insert. We have previously shown the absence of differences in transfection efficacy between wild-type (WT) and mutant MCT8 expression vectors (Jansen et al. 2007). Positions of the mutations are determined using the NM_006517.3 reference

sequence, which uses +1 as the A of the ATG translation initiation codon of the long MCT8 translational isoform, with the initiation codon as codon 1.

Cell culture and transfection

JEG-3 human choriocarcinoma (CVCL_0363) and COS-1 African green monkey kidney cells (CVCL_0223), obtained from ECACC (Sigma-Aldrich), were cultured under standard conditions (Groeneweg et al. 2018). For uptake studies, COS-1 or JEG-3 cells were seeded in 24-well plates and transiently transfected with 100 ng empty vector, or wild-type or mutant MCT8 alone, or in combination with 50 ng CRYM. For immunoblotting, cells were seeded in 6-well plates and transfected with 500 ng empty vector control, or WT or mutant MCT8. For immunocytochemistry studies, cells were cultured on 20 mm glass coverslips coated with poly-D-lysine (Sigma-Aldrich) and transfected with 100 ng wild-type or mutant MCT8. X-tremeGENE 9 (Roche Diagnostics, Almere, NL) was used as a transfection reagent according to manufacturer's protocol and all transfections were carried at 70% cellular confluence. All experiments have been performed 48 h after transfection. Patient-derived fibroblasts were cultured as previously described (Groeneweg et al. 2018).

TH uptake studies

T3 and T4 uptake studies were conducted as previously described (Groeneweg et al. 2014). Briefly, cells were washed with incubation medium (Dulbecco's phosphate buffered saline with 0.9 mmol/L MgCl2 and 0.5 mmol/L CaCl2 supplemented with 0.1% BSA and 0.1% D-glucose), and subsequently incubated for 30 min at 37 °C with 1 nM (50,000 cpm) [125I]T3 or [125I]T4 in 0.5 ml incubation medium. After incubation, cells were briefly washed with incubation medium and lysed with 0.1 M NaOH. Radioactivity in the cell lysates was measured with a -counter. T3 uptake levels in fibroblasts were adjusted for total protein levels measured by Bradford assay according to manufacturer's guideline (Bio-Rad).

Immunoblotting

Two days after transfection, cells were rinsed with D-PBS, collected in 100 mM sodium phosphate, 2 mM EDTA, pH 7.2 (P100E2) containing protease inhibitor cocktail (Roche Diagnostics), and sonicated on ice. After incubation for 10 min at 70 °C in the presence of 1x NuPAGE 1x lithium dodecyl sulfate loading buffer, 15 μg of total lysate was separated on a 4%–20% gradient Mini-PROTEAN TGX Precast Protein Gel, blotted on polyvinylidene difluoride membranes, blocked with 5% milk and probed overnight at 4 °C with N-terminal MCT8 antibody (dilution 1:20 000). GAPDH (antibody dilution 1:20 000) was used as a loading control. MCT8 and GAPDH were visualized as previously described (Groeneweg et al. 2017a). Expression levels of WT and mutant MCT8 proteins were quantified by densitometry using ImageJ and adjusted for GAPDH expression levels.

Immunocytochemistry

Immunocytochemistry was essentially carried out as previously described (Groeneweg et al. 2014). Briefly, cells were fixed with 4% paraformaldehyde, and permeabilized with 0.2% triton X-100 in PBS. Samples were blocked for 1 h at RT in PBS containing 2% BSA, and incubated overnight with rabbit anti-MCT8 (1:1,000) and mouse monoclonal ZO-1 antibody (RRID:AB_2533147; 1:500). After secondary staining with goat antirabbit Alexa Fluor 488 (1:1000) and goat antimouse Alexa 633 (1:1000), cover slips were mounted on glass slides with Prolong Gold containing DAPI (Invitrogen) and examined on a Zeiss Meta 510 microscope, using Zeiss LSM software (Zeiss NL, Sliedrecht, NL).

Ethical considerations

Skin fibroblasts were kindly provided by care-giving physicians and concerned stored samples that were previously collected for diagnostic purposes. Written informed consent was obtained from the parents or legal representatives of the involved patients and controls. This study was conducted in agreement with the Medical Research Involving Human Subjects Act was carried out through routine diagnostic activity; formal ethics review was therefore not requested by our institutional ethical committee.

Statistics

All statistical analyses were performed as indicated in the Figure legends using GraphPad Prism Version 5 software (GraphPad Software Inc., San Diego, USA). Statistically significant differences are indicated as described in the legends of the corresponding Figures.

This study adheres to the principle of the Helsinki Declaretion and was carried out through routine diagnostic activity; all families provided written informed consent for clinical and genetic testing and their publication according to the Italian bioethics laws.

Case reports (Table 1)

Patient 1 A 29-years old man, who had been previously diagnosed with cerebral palsy, presented to our clinic for a second opinion of his neurological condition. He was the third child (two previous healthy sisters) of non-consanguineous healthy Italian parents. His maternal uncle suffered from an

Table 1 Clinical characteristics. Overview of clinical and developmental characteristics at time the patients came to our attention

	Patient 1	Patient 2
Current age	29 y	12 y
Mutation	c.715A > C, p.Thr239Pro	c.1625 T > C, p.Leu543Pro
Age at onset symptoms	first months of life	first months of life
Weight in kg (percentile)	45(<P3, 28y)	21 (P25, 7y)
Head circumference in cm (percentile, age)	na	52 (P25–50, 7y)
Feeding problems	+	–
Muscle wasting	+	–
Signs of peripheral thyrotoxicosis	–	elevated heart rate (127 bpm)
Hypotonia	+	–
Pyramidal signs	+	mild
Extrapyramidal signs	bradykinesia, tremor, dystonic movements of the limbs, hypomimia	slight bradykinesia, hypomimia
Head control (age)	yes (na)	yes (6 m)
Independent sitting (age)	yes (10 m)	yes (16 m)
Ability to walk (age)	yes, with support (6 y)	yes (4 y)
Speech development (age)	first words at 5 y	first words <3 y
Neuromotor Rregression	yes, after the age of 16y	no
Cognitive impairment (IQ)	<45	47
Serum FT3 in pg/ml (normal range)	4.27 pg/mL, (1.71–3.71)	5.39 pg/mL, (1.71–3.71)
Serum FT4 in pg/ml (normal range)	0.73 ng/mL, (0,70-1,48)	0,82 ng/dl (0,70-1,48)
Serum TSH in mU/l (normal range)	normal	1,52 mIU/L (0,45-3,50)
Clinically evident seizures	no	no
EEG	na	4y: high voltage spike-waves during IPS; 7y: bilateral temporal EDs during drowsiness and sleep
MRI (age performed)	29 y: normal myelination, pallidal calcification	delayed myelination at 11.5 m, normal at 4.5 and 7 y

EDs epileptiform discharges, *EEG* electroencephalogram, *IPS* intermittent photic stimulation, *m* months, *MRI* magnetic resonance imaging, *Na* not available, *p* percentile, *SD* standard deviation, *y* years

undiagnosed early onset encephalopathy with severe intellectual disability, had no speech development, and was wheelchair-dependent. The patient was born after an uneventful pregnancy and delivery. From the first months of life diffuse hypotonia, feeding difficulties and developmental delay became evident. He achieved trunk control at 10 months of age, he was able to stand at 4 years and walk with support since 6 years of age; he pronounced his first words at 5 years of age. During infancy, startle reactions in response to even mild sensory stimuli were reported. The clinical picture had initially remained stable, but from 16 years of age it started to slowly deteriorate. Initially, he only needed a wheelchair to cover long distances, but from the age of 20 years he became wheelchair dependent. Dysarthria also worsened and his speech, which was limited to some words, or short sentences of 2–3 words, became less clear. At 29 years of age, neurological examination revealed diffuse muscular hypotrophy, severe scoliosis, pyramidal (peripheral hypertonia, brisk reflexes, clonus, joint contractures) and extrapyramidal signs (bradykinesia, mild dystonic movements of the limbs and resting and action tremor). He had a moderate cognitive impairment (Wechsler Adult Intelligence Scale- WAIS-R performance quotient <45, other scales not conducted; Raven CPM <5° percentile), but he graduated from secondary school with assistance. His facies was hypomimic and some minor dysmorphisms were observed (bitemporal narrowing, large protruding lower lip, macroglossia, and a high and narrow palate). He had a poor weight gain (45 kg, < -2SD). No dysphagia was reported.

Magnetic Resonance Imaging (MRI) was performed at 29 years of age and revealed no significant white matter abnormalities (Fig. 1). Pallidal T2 hypo-intensities were observed, which were designated as calcifications by a CT scan. A calcium-phosphorus metabolism check-up only showed a marginal deficit of vitamin D, with calcium and phosphate concentrations in the normal range.

Thyroid function tests had been performed at the age of 28 years as part of a routine evaluation of the global hypotrophy and demonstrated elevated free T3 (4,27 pg/dL, normal values 1,71-3,71), slightly reduced free (F)T4 (0.73 ng/dL, normal values 0,7-1,48), and normal TSH concentrations. Because of the characteristic thyroid hormone

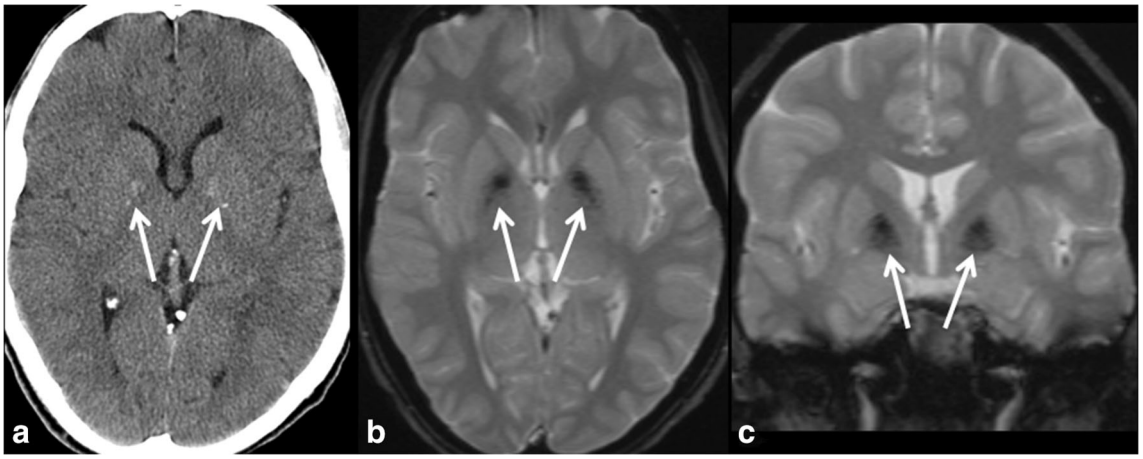

Fig. 1 Brain CT (**a**) and T2 FFE MRI (**b**, **c**) of patient 1 at 29 years of age demonstrating calcifications in both globus pallidus (arrow); note the blooming effect on T2FFE

profile, direct sequencing of the *SLC16A2* gene was performed and revealed a novel hemizygous c.715A > C missense mutation in exon 2, causing a p.Thr239Pro substitution in the MCT8 protein. This mutation was predicted to have a (probable) pathogenic effect on the MCT8 protein by PolyPhen-2 and SIFT. The mother was heterozygous for the same mutation.

Patient 2 A 12-years old patient presented to our clinic at the age of 11 months for a diagnostic work-up of developmental delay. He was the second child born from non-consanguineous Italian parents, after an uneventful pregnancy and cesarean section delivery. The mother declared she had received L-thyroxine for hypothyroidism during pregnancy, and later she underwent a right hemi-thyroidectomy. During the first years of life, he presented neuro-developmental delay: head control was achieved at 6 months, trunk control at 16 months, standing position at 20 months, walking without support since 41 months of age, walking up and down the stairs with aid since 4 years, and first words were pronounced before 36 months. The neurological picture was dominated by cognitive impairment. This was accompanied by moderate truncal hypotonia, subtle pyramidal (brisk reflexes, Babinski and bilateral ankle clonus) and mild extrapyramidal signs (slight bradykinesia, hypomimia, but no dystonia). He had moderate intellectual disability (Griffiths Scale performed at 7 years of age: Global Quotient 47), and was able to communicate using short sentences and understand simple tasks.

MRI of the brain demonstrated a-specific delay of myelination at the age of 11.5 months and was normal at the age of 4.5 and 7 years (Fig. 2).

Since the first exam at the age of 11 months, electroencephalography showed poor and slow background activity. From the age of 4 years, also diffuse high voltage spike-waves (10–40 Hz) were observed during photic stimulation. From the age of 7 years, bilateral temporal epileptiform discharges during drowsiness and sleep were evident. However, he never suffered from clinically evident epileptic seizures. Electroneurography, sensory and visual evoked potential, and electromyography were all unremarkable (last evaluation performed at 7 years).

Biochemical investigations, including urine and plasma guanidinoacetic acid and creatine dosage, lactate and pyruvate, urinary orgnic, acids, plasma and urinary aminoacids, urinary mucopolysaccharides, B12 vitamine and folate, Beta-Galactosidase, Beta-N Acetyl Glucosaminidase), and targeted genetic analysis including karyotyping, fish analyses of subtelomeric regions, a CGH array, and the methylation status of 15q11.2 for Angelman Syndrome were all unremarkable. Only thyroid function tests were found abnormal at 7 years of age and revealed elevated serum free T3 concentrations (5,39 pg/dL normal values 1,71-3,71), and low-normal FT4 (0,82 ng/dl, normal values 0,70-1,48) and TSH (1,52 mIU/L normal values 0,45-3,50) concentrations. Direct sequencing of the *SLC16A2* gene was therefore performed and revealed a novel hemizygous c.1625 T > C missense mutation in exon 6 which results in a p.Leu543Pro substitution in the MCT8 protein, inherited from the mother. This mutation was predicted to have a (probable) pathogenic effect on the MCT8 protein by PolyPhen-2 and SIFT.

Functional analyses

Since both mutations had not been reported before, functional analyses were conducted to confirm their pathogenicity. First the p.Thr239Pro and p.Leu543Pro mutations were introduced into the MCT8 expression construct. In addition, both residues were substituted by an Ala to evaluate if the original Thr239 and Leu543 residues are critical for MCT8 function. In COS-1 cells co-transfected with the intracellular TH-binding protein mu-Crystallin (CRYM), T3 and T4 uptake by the p.Thr239Pro mutant amounted up to 40% of WT, and the

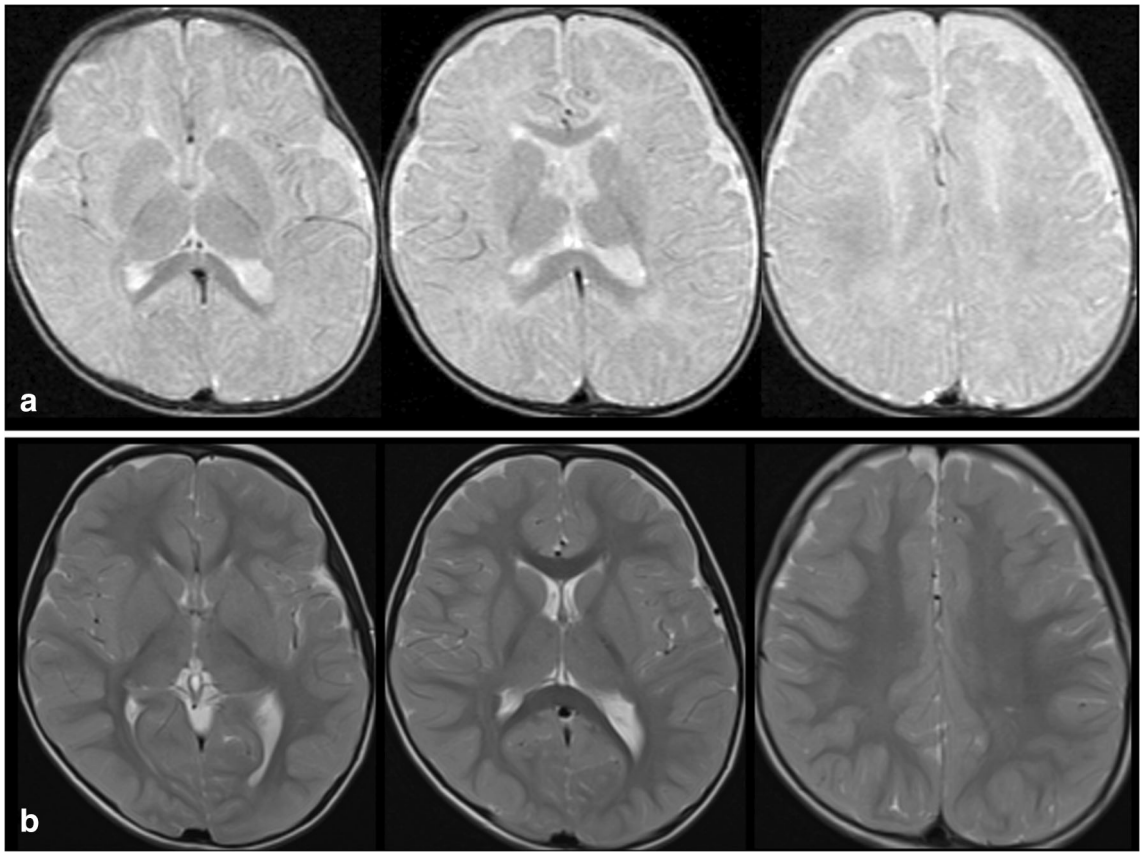

Fig. 2 Brain MRI, T2-w.i. at 11,5 months (TOP) and at 4,5 years (BOTTOM) show delayed myelination at 1 years and the myelination progression until normal appearance at 4,5 years

T3 and T4 uptake by the p.Leu543Pro mutant to 50% of WT MCT8 (Fig. 3a). TH uptake by the p.Thr239Ala and p.Leu543Ala mutants was not significantly different from WT. Similar results were obtained in JEG-3 cells, although residual uptake capacity was slightly lower with 10% for the p.Thr239Pro mutant and 20% for the p.Leu543Pro mutant (Fig. 3b). Saturation experiments in the absence of CRYM revealed an apparent IC_{50} of 18.2 (±1.2) μM for WT MCT8 (Fig. 3c). A similar IC_{50} was found for the p.Thr239Pro mutant (16.9 ± 1.4), whereas the IC50 for the p.Leu543Pro mutant was slightly reduced (9.3 ± 1.2 μM). Immunoblotting on total lysates of COS-1 cell transiently transfected with WT or mutant MCT8 revealed that the protein expression levels of the p.Thr239Ala and p.Leu543Ala mutants were similar to WT, whereas those of p.Thr239Pro and p.Leu543Pro were moderately reduced (Fig. 3d). Similar results were obtained in JEG-3 cells (data not shown). Subcellular localization studies in JEG-3 cells by confocal microscopy showed prominent cell membrane expression of WT (Fig. 3e), whereas a large fraction of the p.Thr239Pro and p.Leu543Pro mutant protein was localized intracellularly and accumulated around the nucleus (Fig. 3e). Both Ala substituents showed a similar subcellular distribution pattern as WT (data not shown). Taken together, these data suggest that both mutations reduce MCT8-mediated TH transport, predominantly by reducing protein expression levels and interference with the intracellular trafficking. This was further supported by our structural model of MCT8 in the outward-open conformation (Groeneweg et al. 2017a, b), in which both residues are located within an a-helical part of transmembrane domain 2 (Thr239) and 11 (Leu543), respectively (Fig. 3f). The introduction of a Pro at these positions likely results in pronounced structural changes of these domains.

In addition to these in vitro studies in over-expressing cells, we also studied the impact of both mutations on MCT8-mediated T3 transport in patient-derived fibroblasts, a well-established ex vivo model to study MCT8 deficiency. As a control we also included fibroblasts from a patient harboring a frameshift mutation that truncates the MCT8 protein prematurely, resulting in a complete loss of MCT8-mediated T3 uptake (Groeneweg et al. 2018). In line with the in vitro studies, the p.Thr239Pro and p.Leu543Pro mutant fibroblasts showed a significant reduction in T3 uptake compared to fibroblasts derived from healthy controls at all tested time points, but exceeded those observed in Q97fsX mutant fibroblasts (Fig. 1g). In addition, MCT8 protein expression levels were clearly lower in the p.Thr239Pro and p.Leu543Pro mutant fibroblasts compared to control fibroblasts (Fig. 3h).

Finally, T3 uptake by patient and control fibroblasts was measured in the absence and presence of the MCT8-specific inhibitor silychristin (Johannes et al. 2016). In the presence of silychristin, T3 uptake levels in control fibroblasts were diminished by about 70%, whereas no reduction was observed in the Q97fsX fibroblasts corresponding to a complete loss of MCT8 function (Fig. 3i). In contrast, T3 uptake was moderately reduced by silychristin in p.Thr239Pro (~16%) and p.Leu543Pro (~49%) mutant fibroblasts, indicating the presence of some residual MCT8-mediated T3 uptake.

Discussion

Here, we report two novel mutations in the *SLC16A2* gene (p.Thr239Pro and p.Leu543Pro), resulting in a less severe clinical phenotype of MCT8 deficiency. Although both patients were able to walk and developed some speech, neuromotor development was considerably better in the one harboring the p.Leu543Pro mutation. In vitro and ex vivo studies confirmed that both mutations resulted in a reduction of MCT8 function. In line with the less severe clinical phenotype, a relatively higher residual transport capacity was observed for the p.Leu543Pro mutant.

To date, up to a hundred different genetic mutations in MCT8 have been reported and for the majority of patients with MCT8 deficiency at least some aspects of the clinical phenotype have been described (reviewed in (Groeneweg et al. 2017b)). With the growing number of identified patients, the presence of heterogeneity in the severity of the clinical phenotype has become increasingly clear. The majority of patients reported has severe intellectual disability and are unable to sit or stand without support, but a subset of patients is able to walk and talk in simple words (Stevenson et al. 1990; Schwartz et al. 2005; Vaurs-Barriere et al. 2009; Visser et al. 2009; Novara et al. 2017). Regardless the severity of the clinical phenotype, the presence of abnormal thyroid function tests appears to be a consistent finding, with serum T3 concentration being elevated, free and total T4 concentrations reduced and TSH concentrations mostly within normal range.

Early diagnosis of patients with a clinical phenotype in the milder spectrum of MCT8 deficiency is often challenging and complicated by initial misclassification. This was also the case with our two patients who both presented a relatively mild clinical phenotype. The first patient (p.Thr239Pro) presented as a non-progressive encephalopathy with intellectual disability, and pyramidal and extrapyramidal signs. Despite a normal perinatal history, he had been initially diagnosed with cerebral palsy. The second patient (p.Leu543Pro) mainly presented with cognitive delay. A congenital static neurodevelopmental encephalopathy had been considered the most probable diagnostic hypothesis. Although both patients presented classical clinical hallmarks of MCT8 deficiency, including early hypotonia, pyramidal and extrapyramidal signs, intellectual disability and slightly abnormal myelination (only proband 2), these features were so mild to make them considered as a-specific and the diagnosis of MCT8 deficiency was therefore initially not deemed very likely. Moreover, beside the low body weight and muscular hypotrophy in patient 1, and an elevated heart rate in patient 2, both of them did not have other obvious clinical signs of peripheral hyperthyroidism. The presence of abnormal thyroid function tests finally led to the correct diagnosis.

Although the elevated T3 concentrations are an important clue for the diagnosis of MCT8 deficiency, they are not routinely measured or unavailable in clinical practice. The evaluation of thyroid function tests is often restricted to TSH, sometimes accompanied with FT4, the results of which are regularly misinterpreted as central hypothyroidism. Consequently, some patients are treated with levothyroxine supplementation, which in fact may further deteriorate the thyrotoxicosis in the peripheral tissues and worsen the peripheral phenotype (e.g. (de Menezes-Filho et al. 2011, Kim et al. 2015)). Therefore, the additional measurement of T3 in male subjects with global developmental delay should be routinely considered.

In agreement with the relatively mild clinical presentation, both identified mutations resulted in a mutant MCT8 protein with considerable residual TH transport capacity. In vitro studies in overexpressing COS-1 cells showed residual uptake functions of 40% for the p.Thr239Pro mutant and 50% for the p.Leu543Pro mutant, which is similar to the levels reported for other mutations identified in patients with a less severe phenotype (e.g.(Visser et al. 2009)). Also, the ex vivo experiments in patient fibroblasts indicated that both mutant proteins have significant residual transport capacity. Our findings are in line with previous studies that have suggested that the severity of the clinical phenotype is related to the residual transport capacity of the mutant MCT8 protein in functional studies (e.g. (Capri et al. 2013, Novara et al. 2017)). Additional in vitro studies, suggested that both mutations reduce the stability of the MCT8 protein, resulting in lower protein expression levels and more pronounced perinuclear subcellular localization compared to wild-type. The latter may indicate an impaired trafficking of both mutant proteins to the cell membrane. Since both residues are predicted to be located within a transmembrane domain with an alpha-helical structure, the helix-breaking properties of a Pro likely result in disorganization of the secondary protein structure. Indeed, substitution of Thr239 or Leu543 by an Ala, which has a small side-chain and backbone properties that allow incorporation in an alpha-helical structure, resulted in mutant proteins with a TH transport activity similar to WT. These findings also suggest that the Thr239 and Leu543 themselves are not strictly essential for MCT8 function and that the introduction of a Pro at these positions likely mediates the pathogenic effects of both identified mutations.

Of interest, the neuroradiological evaluation of patient 1 at 29 years of age showed the presence of bilateral pallidal calcifications. This feature has been mentioned in only two

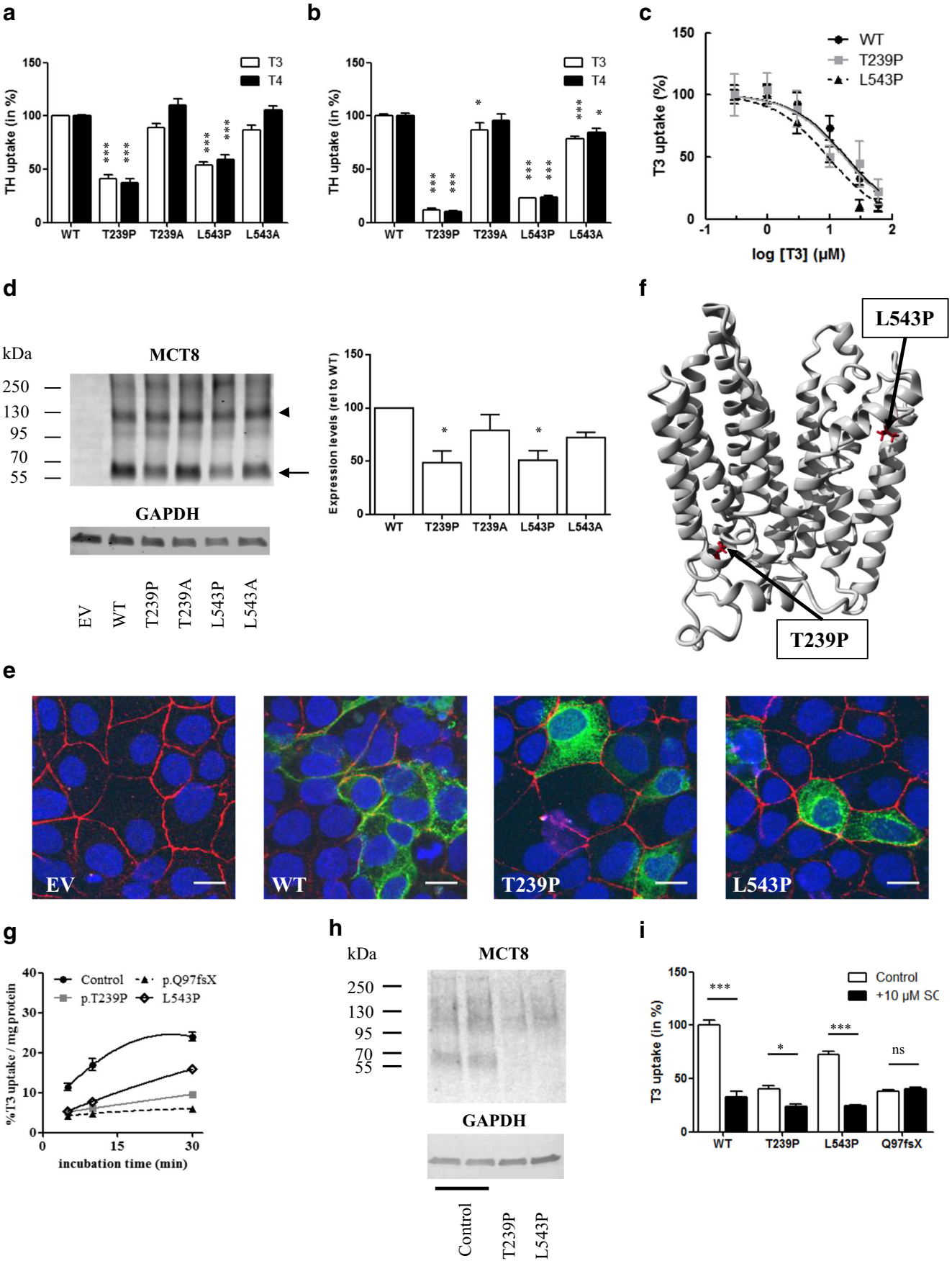
a
TH uptake (in %)
T3
T4
WT
T239P
T239A
L543P
L543A
b
TH uptake (in %)
c
T3 uptake (%)
log [T3] (μM)
WT
T239P
L543P
d
kDa
MCT8
250
130
95
70
55
GAPDH
EV
WT
T239P
T239A
L543P
L543A
Expression levels (rel to WT)
f
L543P
T239P
e
EV
WT
T239P
L543P
g
Control
p.Q97fsX
p.T239P
L543P
%T3 uptake / mg protein
incubation time (min)
h
kDa
MCT8
GAPDH
Control
T239P
L543P
i
T3 uptake (in %)
Control
+10 μM SC
WT
T239P
L543P
Q97fsX
ns

◀ **Fig. 3** Functional analyses of the p.Thr239Pro and p.Leu543Pro mutants in in vivo and ex vivo disease models for MCT8 deficiency. T3 (white bars) and T4 (black bars) uptake in COS-1 (**a**) and JEG-3 (**b**) cells transiently transfected with WT MCT8 or indicated mutants in the presence of the intracellular TH-binding protein CRYM, after 30 min at 37 °C. Uptake levels were corrected for those observed in empty vector (EV) transfected cells and expressed relative to WT (100%; $N = 3$). One-way ANOVA with Bonferroni posthoc tests were used and statistically significant differences to WT are indicated as follows $P < 0.001$, ***, $P < 0.05$, *. **c** Saturation experiments in transiently transfected COS-1 cells in the absence of CRYM, corrected for background uptake levels observed in cell transfected with EV. Non-linear regression was used to plot the saturation curves. IC50 values for WT (18.2, 95% confidence interval [CI] 12.4–26.7 μM), p.Thr239Pro (16.9, 95%CI 8.6–33.1 μM) and p.Leu543Pro (9.3, 95% CI 6.2–14.0 μM) mutant MCT8 were calculated based on the means of N = 3 independent experiments using GraphPad Prism. **d** Immunoblot on total lysates of COS-1 cells transiently transfected with WT or mutant MCT8. MCT8 monomer is indicated with an arrow and MCT8 homo-dimer with an arrowhead. Glyceraldehyde-3-phosphate dehydrogenase (GAPDH) was used as loading control. The expression levels of wildtype and indicated mutant MCT8 proteins has been quantified using ImageJ and adjusted for GAPDH levels. All levels are expressed relative to WT MCT8 and presented as mean ± SEM of 3 independent experiments. One-way ANOVA followed by a Bonferroni multiple-comparison test was used to compare the expression levels of all tested mutants to WT MCT8. * denote statistically significant differences ($p < 0.05$). **e** Confocal microscopy in transiently transfected JEG-3 cells using antibodies against MCT (green), the membrane marker ZO-1 (red) and the nuclear marker DAPI (blue), presented as an overlay image. **f** Structural homology model of MCT8 in the outwardopen configuration (25) in which the position of the affected Thr239 and Leu543 have been indicated. **g** T3 uptake in patient and control fibroblasts after indicated incubation times at 37 °C. T3 uptake levels are presented as mean ± SEM percentage internalized T3 per milligram protein to correct for differences in cell density between different fibroblast lines. T3 uptake in fibroblasts derived from patients with MCT8 deficiency was significantly lower than in those obtained from healthy controls (mean of 2 different control cell lines) at all tested incubation times (One-way ANOVA with Bonferroni post-hoc tests: $P < 0.001$ at all time-points, not indicated in graph). **h** MCT8 expression levels in patient and control fibroblasts. **i** T3 uptake levels in patient and control fibroblasts in the absence (−) or presence (+) of 10 μM silychristin (SC). Silychristin is a potent and, thus far the most specific, inhibitor of MCT8-mediated TH transport (26). The silychristin-induced reduction in T3 uptake in all patient lines was significantly smaller (One-way ANOVA with Bonferroni posthoc tests, $P < 0.05$) than in control fibroblasts

previously described patients (Ono et al. 2016; Dumitrescu et al. 2004) but left unattended ever since. In one case, calcium deposits were found during autopsy at the age of 10 years (Dumitrescu et al. 2004), and in another T1 shortening signals considered suggestive for calcification, were detected in the bilateral globus pallidus and dentate nucleus at the age of 21 years (Ono et al. 2016). Since brain imaging at these relatively advanced ages is not routinely performed in patients with MCT8 deficiency, it is currently not known to what extent calcifications in the basal ganglia are present at the pediatric age. This in particular holds for CT imaging of the brain which is the preferred detection method for cerebral calcifications. Of note, the presence of calcifications of the basal ganglia has been reported in patients with neural cretinism (Halpern et al. 1991) and (congenital) hypothyroidism (Arii et al. 2002), which may suggest a link between the abnormal TH signaling in the brain and this phenomenon. Nevertheless, it remains unclear if the presence of calcifications in the basal ganglia at a relatively young age is a common feature in patients with MCT8 deficiency, and if it is directly related to the aberrant TH signaling in the brain or to premature (para-) physiological calcification that normally occurs with aging. Alternative causes were excluded in our patient. More detailed neuroradiological studies in patients at different ages are needed to further elucidate the etiology of this finding. Should (premature) calcifications of the basal ganglia be directly related to the defect in TH signaling, our finding may suggest that besides the developmental defects associated with MCT8 deficiency, additional pathological changes may occur later in life.

Finally it is to note that in both patients extrapyramidal signs manifested as bradykinesia and hypomimia, while dystonia was only mild or even absent. Dystonia has been often reported as the main extrapyramidal feature of MCT8 patients (Matheus et al. 2015), but it has already pointed out that this is not constantly present, as our cases (La Piana et al. 2015).

In conclusion, we reported on two novel mutations in *SLC16A2* which are associated with clinical features at the milder side of the spectrum of MCT8 deficiency. Our cases illustrate that a timely diagnosis of such patients can be challenging and prone to misclassification. We therefore advocate to measure thyroid function tests, including serum T3 concentrations, in the work-up of patients with X-linked intellectual disability, even when the typical neurological and neuroradiological signs of MCT8 deficiency are only subtle and apparently a-specific.

Acknowledgements We thank Ramona E.A. van Heerebeek and Selmar Leeuwenburgh for the technical assistance, the Optical Imaging Center (Erasmus Medical Center Rotterdam) for technical support regarding the confocal imaging studies, and the physicians of the involved patients and healthy controls for providing the fibroblasts.

Financial support This work was supported by a grant from the Netherlands Organisation for Health Research and Development (project number 113303005) (to WEV), from the Sherman Foundation (to WEV).

Compliance with ethical standards

Conflict of interest All authors declare no conflict of interest.

Disclosure statement The authors have nothing to disclose.

References

Arii J, Tanabe Y, Makino M, Sato H, Kohno Y (2002) Children with irreversible brain damage associated with hypothyroidism and multiple intracranial calcifications. J Child Neurol 17(4):309–313. https://doi.org/10.1177/088307380201700416

Capri Y, Friesema EC, Kersseboom S, Touraine R, Monnier A, Eymard-Pierre E, Des Portes V, De Michele G, Brady AF, Boespflug-Tanguy O, Visser TJ, Vaurs-Barriere C (2013) Relevance of different cellular models in determining the effects of mutations on SLC16A2/MCT8 thyroid hormone transporter function and genotype-phenotype correlation. Hum Mutat 34(7):1018–1025. https://doi.org/10.1002/humu.22331

de Menezes-Filho HC, Marui S, Manna TD, Brust ES, Radonsky V, Kuperman H, Dichtchekenian V, Setian N, Damiani D (2011) Novel mutation in MCT8 gene in a Brazilian boy with thyroid hormone resistance and severe neurologic abnormalities. Arq Bras Endocrinol Metabol 55(1):60–66. https://doi.org/10.1590/S0004-27302011000100008

Dumitrescu AM, Liao XH, Best TB, Brockmann K, Refetoff S (2004) A novel syndrome combining thyroid and neurological abnormalities is associated with mutations in a monocarboxylate transporter gene. Am J Hum Genet 74(1):168–175. https://doi.org/10.1086/380999

Friesema EC, Ganguly S, Abdalla A, Manning Fox JE, Halestrap AP, Visser TJ (2003) Identification of monocarboxylate transporter 8 as a specific thyroid hormone transporter. J Biol Chem 278(41):40128–40135. https://doi.org/10.1074/jbc.M300909200

Friesema EC, Grueters A, Biebermann H, Krude H, von Moers A, Reeser M, Barrett TG, Mancilla EE, Svensson J, Kester MH, Kuiper GG, Balkassmi S, Uitterlinden AG, Koehrle J, Rodien P, Halestrap AP, Visser TJ (2004) Association between mutations in a thyroid hormone transporter and severe X-linked psychomotor retardation. Lancet 364(9443):1435–1437. https://doi.org/10.1016/S0140-6736(04)17226-7

Friesema EC, Kuiper GG, Jansen J, Visser TJ, Kester MH (2006) Thyroid hormone transport by the human monocarboxylate transporter 8 and its rate-limiting role in intracellular metabolism. Mol Endocrinol 20(11):2761–2772. https://doi.org/10.1210/me.2005-0256

Friesema EC, Jansen J, Jachtenberg JW, Visser WE, Kester MH, Visser TJ (2008) Effective cellular uptake and efflux of thyroid hormone by human monocarboxylate transporter 10. Mol Endocrinol 22(6):1357–1369. https://doi.org/10.1210/me.2007-0112

Gereben B, Zavacki AM, Ribich S, Kim BW, Huang SA, Simonides WS, Zeold A, Bianco AC (2008) Cellular and molecular basis of deiodinase-regulated thyroid hormone signaling. Endocr Rev 29(7):898–938. https://doi.org/10.1210/er.2008-0019

Groeneweg S, Friesema EC, Kersseboom S, Klootwijk W, Visser WE, Peeters RP, Visser TJ (2014) The role of Arg445 and Asp498 in the human thyroid hormone transporter MCT8. Endocrinology 155(2):618–626. https://doi.org/10.1210/en.2013-1521

Groeneweg S, Peeters RP, Visser TJ, Visser WE (2016) Diagnostic and therapeutic challenges in the Allan–Herndon–Dudley syndrome. US Endocrinology 12(2):90–93. https://doi.org/10.17925/USE.2016.12.02.90

Groeneweg S, Lima de Souza EC, Meima ME, Peeters RP, Visser WE, Visser TJ (2017a) Outward-Open Model of Thyroid Hormone Transporter Monocarboxylate Transporter 8 Provides Novel Structural and Functional Insights. Endocrinology 158(10):3292–3306. https://doi.org/10.1210/en.2017-00082

Groeneweg S, Visser WE, Visser TJ (2017b) Disorder of thyroid hormone transport into the tissues. Best Pract Res Clin Endocrinol Metab 31(2):241–253. https://doi.org/10.1016/j.beem.2017.05.001

Groeneweg S, van den Berge A, Meima ME, Peeters RP, Visser TJ, Visser WE (2018) Effects of chemical chaperones on thyroid hormone transport by MCT8 mutants in patient-derived fibroblasts. Endocrinology 159(3):1290–1302. https://doi.org/10.1210/en.2017-00846

Halpern JP, Boyages SC, Maberly GF, Collins JK, Eastman CJ, Morris JG (1991) The neurology of endemic cretinism. A study of two endemias. Brain 114(Pt 2):825–841

Hennemann G, Docter R, Friesema EC, de Jong M, Krenning EP, Visser TJ (2001) Plasma membrane transport of thyroid hormones and its role in thyroid hormone metabolism and bioavailability. Endocr Rev 22(4):451–476. https://doi.org/10.1210/edrv.22.4.0435

Jansen J, Friesema EC, Kester MH, Milici C, Reeser M, Gruters A, Barrett TG, Mancilla EE, Svensson J, Wemeau JL, Busi da Silva Canalli MH, Lundgren J, McEntagart ME, Hopper N, Arts WF, Visser TJ (2007) Functional analysis of monocarboxylate transporter 8 mutations identified in patients with X-linked psychomotor retardation and elevated serum triiodothyronine. J Clin Endocrinol Metab 92(6):2378–2381. https://doi.org/10.1210/jc.2006-2570

Johannes J, Jayarama-Naidu R, Meyer F, Wirth EK, Schweizer U, Schomburg L, Kohrle J, Renko K (2016) Silychristin, a Flavonolignan derived from the Milk thistle, is a potent inhibitor of the thyroid hormone transporter MCT8. Endocrinology 157(4):1694–1701. https://doi.org/10.1210/en.2015-1933

Kim JH, Kim YM, Yum MS, Choi JH, Lee BH, Kim GH, Yoo HW (2015) Clinical and endocrine features of two Allan-Herndon-Dudley syndrome patients with monocarboxylate transporter 8 mutations. Horm Res Paediatr 83(4):288–292. https://doi.org/10.1159/000371466

La Piana R, Vanasse M, Brais B, Bernard G (2015) Myelination delay and Allan-Herndon-Dudley syndrome caused by a novel mutation in the SLC16A2 gene. J Child Neurol 30(10):1371–1374. https://doi.org/10.1177/0883073814555189

Matheus MG, Lehman RK, Bonilha L, Holden KR (2015) Redefining the pediatric phenotype of X-linked Monocarboxylate transporter 8 (MCT8) deficiency: implications for diagnosis and therapies. J Child Neurol. https://doi.org/10.1177/0883073815578524

Mayerl S, Muller J, Bauer R, Richert S, Kassmann CM, Darras VM, Buder K, Boelen A, Visser TJ, Heuer H (2014) Transporters MCT8 and OATP1C1 maintain murine brain thyroid hormone homeostasis. J Clin Invest 124(5):1987–1999. https://doi.org/10.1172/JCI70324

Mol JA, Visser TJ (1985) Synthesis and some properties of sulfate esters and sulfamates of iodothyronines. Endocrinology 117(1):1–7. https://doi.org/10.1210/endo-117-1-1

Novara F, Groeneweg S, Freri E, Estienne M, Reho P, Matricardi S, Castellotti B, Visser WE, Zuffardi O, Visser TJ (2017) Clinical and molecular characteristics of SLC16A2 (MCT8) mutations in three families with the Allan-Herndon-Dudley syndrome. Hum Mutat 38(3):260–264. https://doi.org/10.1002/humu.23140

Ono E, Ariga M, Oshima S, Hayakawa M, Imai M, Ochiai Y, Mochizuki H, Namba N, Ozono K, Miyata I (2016) Three novel mutations of the MCT8 (SLC16A2) gene: individual and temporal variations of endocrinological and radiological features. Clin Pediatr Endocrinol 25(2):23–35. https://doi.org/10.1297/cpe.25.23

Schwartz CE, May MM, Carpenter NJ, Rogers RC, Martin J, Bialer MG, Ward J, Sanabria J, Marsa S, Lewis JA, Echeverri R, Lubs HA, Voeller K, Simensen RJ, Stevenson RE (2005) Allan-Herndon-Dudley syndrome and the monocarboxylate transporter 8 (MCT8) gene. Am J Hum Genet 77(1):41–53. https://doi.org/10.1086/431313

Stevenson RE, Goodman HO, Schwartz CE, Simensen RJ, McLean WT Jr, Herndon CN (1990) Allan-Herndon syndrome. I. Clinical studies. Am J Hum Genet 47(3):446–453

Tonduti D, Vanderver A, Berardinelli A, Schmidt JL, Collins CD, Novara F, Genni AD, Mita A, Triulzi F, Brunstrom-Hernandez JE, Zuffardi O, Balottin U, Orcesi S (2013) MCT8 deficiency: extrapyramidal symptoms and delayed myelination as prominent features. J Child Neurol 28(6):795–800. https://doi.org/10.1177/0883073812450944

Vatine GD, Al-Ahmad A, Barriga BK, Svendsen S, Salim A, Garcia L, Garcia VJ, Ho R, Yucer N, Qian T, Lim RG, Wu J, Thompson LM, Spivia WR, Chen Z, Van Eyk J, Palecek SP, Refetoff S, Shusta EV, Svendsen CN (2017) Modeling psychomotor retardation using iPSCs from MCT8-deficient patients indicates a prominent role for

the blood-brain barrier. Cell Stem Cell 20(6):831–843 e5. https://doi.org/10.1016/j.stem.2017.04.002

Vaurs-Barriere C, Deville M, Sarret C, Giraud G, Des Portes V, Prats-Vinas JM, De Michele G, Dan B, Brady AF, Boespflug-Tanguy O, Touraine R (2009) Pelizaeus-Merzbacher-like disease presentation of MCT8 mutated male subjects. Ann Neurol 65(1):114–118. https://doi.org/10.1002/ana.21579

Visser WE, Jansen J, Friesema EC, Kester MH, Mancilla E, Lundgren J, van der Knaap MS, Lunsing RJ, Brouwer OF, Visser TJ (2009) Novel pathogenic mechanism suggested by ex vivo analysis of MCT8 (SLC16A2) mutations. Hum Mutat 30(1):29–38. https://doi.org/10.1002/humu.20808

Yen PM (2001) Physiological and molecular basis of thyroid hormone action. Physiol Rev 81(3):1097–1142. https://doi.org/10.1152/physrev.2001.81.3.1097

Yen PM, Ando S, Feng X, Liu Y, Maruvada P, Xia X (2006) Thyroid hormone action at the cellular, genomic and target gene levels. Mol Cell Endocrinol 246(1-2):121–127. https://doi.org/10.1016/j.mce.2005.11.030